Effect of pH on Axial Ligand Coordination of Cytochrome *c″* from *Methylophilus methylotrophus* and Horse Heart Cytochrome *c*†

Chiara Indiani,[‡,§] Giampiero de Sanctis,[‡,||] Francesca Neri,[§] Helena Santos,[⊥] Giulietta Smulevich,*[,§] and Massimo Coletta*[,▽]

Dipartimento di Chimica, Università di Firenze, Via Gino Capponi 9, I-50121 Firenze, Italy, Dipartimento di Biologia Molecolare, Cellulare ed Animale, Università di Camerino, I-62032 Camerino (MC), Italy, Instituto de Tecnologia Quimica e Bioquimica, Universita Nova de Lisboa, Rua da Quinta Grande, Apartado 127, P-2780 Oeiras, Portugal, and Dipartimento di Medicina Sperimentale e Scienze Biochimiche, Università di Roma Tor Vergata, Via di Tor Vergata 135, I-00133 Roma, Italy

Received February 3, 2000; Revised Manuscript Received April 24, 2000

ABSTRACT: The effect of protons on the axial ligand coordination and on structural aspects of the protein moiety of cytochrome *c″* from *Methylophilus methylotrophus*, an obligate methylotroph, has been investigated down to very low pH (i.e., 0.3). The unusual resistance of this cytochrome to very low pH values has been exploited to carry out this study in comparison with horse heart cytochrome *c*. The experiments were undertaken at a constant phosphate concentration to minimize the variation of ionic strength with pH. The pH-linked effects have been monitored at 23 °C in the oxidized forms of both cytochromes by following the variations in the electronic absorption, circular dichroism and resonance Raman spectra. This approach has enabled the conformational changes of the heme surroundings to be monitored and compared with the concomitant overall structural rearrangements of the molecule. The results indicate that horse heart cytochrome *c* undergoes a first conformational change at around pH 2.0. This event is possibly related to the cleavage of the Fe−Met80 bond and a likely coordination of a H_2O molecule as a sixth axial ligand. Conversely, in cytochrome *c″* from *M. methylotrophus*, a variation of the axial ligand coordination occurs at a pH that is about 1 unit lower. Further, it appears that a concerted cleavage of both His ligands takes place, suggesting indeed that the different axial ligands present in horse heart cytochrome *c* (Met/His) and in cytochrome *c″* from *M. methylotrophus* (His/His) affect the heme conformational changes.

The effect of ionic strength and acid denaturation on proteins has been widely investigated and one of the most extensively studied systems is cytochrome *c* from horse heart (hh cyt c). It has been shown to exist in partially folded states depending on the nature of the anions and on their concentration (*1*−*9*). Such studies indicate that pH-dependent transitions at very low pH values are the result of various forces that stabilize or destabilize intermediate state(s) (*10*), defined as A-state(s) or "molten globule" state(s) (*1, 2*). In particular, it has been recently shown that the role of axial ligands appears to be crucial for stabilizing the "molten globule" (*8, 11*), and that His18 (which is the proximal axial heme ligand of hh cyt c) should contribute more than Met80 (the distal axial heme ligand of hh cyt c) to the stabilization of the "molten globule" at low pH.

In this respect, cytochrome *c″* from *Methylophilus methylotrophus* (cyt c″) appears very interesting, since it contains two histidines as axial ligands in the oxidized form (*12, 13*). Therefore, the role of the bis-histidyl coordination of the heme on the stabilization of the intermediate states at low pH values can be studied in this protein. Furthermore, an advantage is represented by the great resistance to denaturation of this protein, as indicated by the full reversibility of the pH-induced structural transition (*14*). In a preliminary study, we have reported that at pH 1.5 the α-helical content decreases by about 60% toward a random coil arrangement (*14*). This conformational change appears to be accompanied by drastic changes in the heme coordination geometry, suggesting that one or both histidines might be detached and the heme becomes penta- and/or tetracoordinated. Moreover, the conformational change induced by low pH leads to a new stable structural arrangement, in which the protein, though likely unfolded to a partial extent, appears still capable of fully recovering the native structure.

The remarkable stability of cyt c″ from *M. methylotrophus* to acid pH values and the full reversibility of all observed structural changes elicited our interest to investigate further

† This work was supported by the Italian Consiglio Nazionale delle Ricerche (CNR) and Ministero della Università e della Ricerca Scientifica e Tecnologica (MURST ex 60%, Cofin Murst 97 CFSIB to G.S. and Cofin 9803184222 to M.C.).

* To whom correspondence should be addressed. M.C.: Telephone +39 0672596365; fax +39 0672596353; e-mail coletta@seneca.uniroma2.it. G.S.: Telephone +39 0552757596; fax +39 0552476961; e-mail smulev@chim.unifi.it.

‡ These authors have equally contributed to this work.

§ Università di Firenze.

|| Università di Camerino.

⊥ Universita Nova de Lisboa.

▽ Università di Roma Tor Vergata.

[1] Abbreviations: hh cyt c, horse heart cytochrome *c*; cyt c″, cytochrome *c″* from *Methylophilus methylotrophus*; RR, resonance Raman; CD, circular dichroism, 5-c and 6-c, 5-coordinate and 6-coordinate; HS, high-spin; LS, low-spin; CT1, long-wavelength (>600 nm) porphyrin-to-metal charge-transfer band.

10.1021/bi000266i CCC: $19.00
Published on Web 06/20/2000

the behavior of this protein at even lower pH values. In the present work we have focused our study on the variations of the axial ligand coordination down to pH 0.3 by means of electronic absorption, circular dichroism, and resonance Raman (RR) spectroscopy. The results are compared with those of hh cyt c obtained under the same conditions.

EXPERIMENTAL PROCEDURE

Cytochrome *c″* from *Methylophilus methylotrophus* was purified as previously reported (*14*). Horse heart cytochrome *c* (type VI) was purchased from Sigma and used without further purification.

Potassium phosphate buffers have been used at various pH values between 7.0 and 0.3 at different concentrations (i.e., 12 mM, 1 M, and 3 M).

Sample concentration was about 0.01−0.04 mM for RR spectroscopy, about 0.05−0.1 mM for UV−visible absorption, and about 0.005−0.05 mM for circular dichroism measurements.

Absorption spectra, recorded with a Cary 5 spectrophotometer, were measured both prior to and after RR measurements. No degradation was observed under the experimental conditions. The RR spectra were obtained by excitation with 406.7 nm line of Kr^+ laser (Coherent, Innova 90/K). The backscattered light from a slowly rotating NMR tube was collected and focused into a computer-controlled double monochromator (Jobin-Yvon HG 2S) equipped with a cooled photomultiplier (RCA C31034 A) and photon counting electronics. The RR spectra were calibrated with indene and CCl_4 as standards to an accuracy of ± 1 cm^{-1} for intense bands. In the figures the relative intensities of the high-frequency RR bands are normalized on the ν_4 band (not shown in the figures). Circular dichroism spectra have been obtained on a Jasco J-700 spectropolarimeter. Results are expressed as mean ellipticity $[\theta]$, which is defined as $[\theta] = 100\theta_{obs}/lc$, where θ_{obs} is the observed ellipticity in degrees, c is the concentration in moles of residue per liter (in the far-UV region) or in moles of heme per liter (in the near-UV and in the Soret region), and l is the path length in centimeters. CD spectra have been obtained with a cuvette of 0.2 or 1 cm (only in the near-UV region) path length.

All the electronic absorption and circular dichroism spectra were collected at room temperature, i.e., at about 23 °C. The RR spectra were collected at approximately 15 °C. The rotating NMR tube was cooled by a gentle flow of N_2 gas passed through liquid N_2 to minimize the local heating of the protein induced by the laser beam.

RESULTS

At very low pH values (i.e., between pH 1.9 and 0.3) it is very difficult to keep constant the ionic strength. This is especially important in view of the documented effect of the ionic strength on the pH-dependent transitions (*8*). Therefore, we have first investigated the effect of phosphate concentration on the spectroscopic features of hh cyt c and cyt c″ at several pH values. Figure 1 shows for both cytochromes the effect of phosphate concentration (i.e., 12 mM, 1 M, and 3 M) at pH 1.9 by CD spectra in the far UV region (panel A) and in the Soret region (panel B), electronic absorption (panel C), and RR spectra (panel D). It has been shown previously that at neutral pH both cytochromes have spectroscopic features typical of six-coordinate low-spin heme (6-c LS), whereas upon lowering the pH to 1.9−1.5 at low ionic strength an increase of the random coil arrangement at the expense of the α-helical content was observed. These changes were accompanied by a marked decrease of the 6-c LS heme and the appearance of both 5- and 6-c high-spin (HS) hemes (*6, 14*). The increase of phosphate concentration brings about the recovery of the axial coordination of the heme observed at higher pH values. Concomitantly, a partial refolding of the native structure of both cytochromes is observed (Figure 1A). Furthermore, the electronic absorption and RR spectra (Figure 1C,D), recorded at the three different phosphate concentrations, do not show any appreciable difference between 1 M and 3 M phosphate buffers, suggesting that the ionic strength-dependent effect is indeed complete at 3 M phosphate. The same behavior is observed at all pH values investigated below pH 1.9 (data not shown). Thus, all experiments were carried out at a constant high phosphate concentration (i.e., 3 M), which is also the value required to attain the lowest pH investigated (i.e., pH 0.3). Although a constant phosphate concentration (i.e., 3 M) over the pH 0.3−1.9 range does not mean a strictly constant ionic strength, these data allow this variation to be considered negligible for the phenomena observed and to drastically reduce the influence of a factor that might have rendered our observations inhomogeneous. The phosphate-dependent spectroscopic behavior is similar for hh cyt c and cyt c″, and it essentially consists of lowering the pK_a of the pH-dependent structural transition to values much lower than those previously reported for cyt *c″* (*14*), shifting the equilibrium toward a less unfolded structure, as previously observed for hh cyt c (*10*).

Figure 2 shows the electronic absorption spectra of oxidized cyt c″ (panel A) and hh cyt c (panel B) upon lowering the pH from 7.0 to 0.3 in 3 M phosphate buffer. At pH 7.0 the spectrum of cyt c″, due to a 6-c LS heme (*14*), is characterized by a Soret maximum at 406 nm and Q-bands at 526 and 553 nm (the latter as a shoulder) (spectrum a in Figure 2A). Similar considerations can be made for hh cyt c, even though the absorption maxima are red-shifted with respect to cyt c″ at neutral pH with the Soret band at 409 nm and Q-bands at 530 and 555 nm (spectrum a in Figure 2B). Lowering the pH below 2 brings about the progressive appearance of new species in both cytochromes with a Soret band at 396 nm (in cyt c″) or 398 nm (in hh cyt c), Q-bands at 500 and 526 nm (in cyt c″) or at 501 and 528 nm (in hh cyt c), and the appearance of a charge-transfer (CT1) band at 625 nm (in cyt c″) or at 624 nm (in hh cyt c). These values differ slightly from those previously reported at lower ionic strength (*14*). The pH-induced changes indicate an increase of high-spin (HS) species at the expense of the low-spin heme observed at higher pH, suggesting that between pH 1.9 and 0.3 at least one of the axial bonds of the heme is cleaved or severely weakened. However, as a whole, no major differences can be observed in the pH-dependent behavior of the UV−visible spectra between the two proteins, except that the transition seems to occur at different pH values in the two cytochromes.

Figure 3 shows the CD spectra, over the same pH range, for cyt c″ (bottom) and hh cyt c (top), respectively, in the far-UV region (panel A), the near-UV region (panel B), and the Soret region (panel C). At pH 7.0, the CD spectra of the

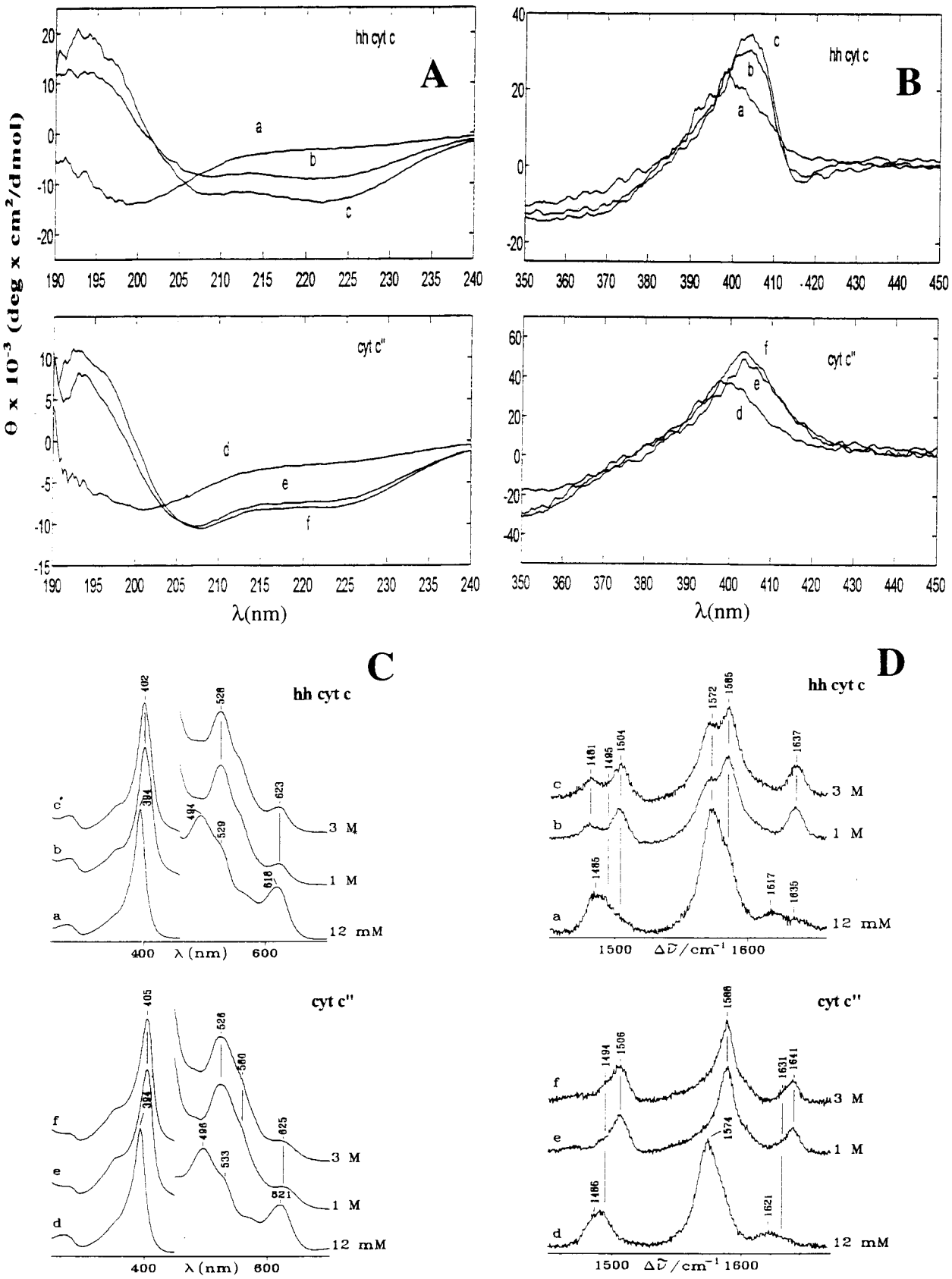

FIGURE 1: Oxidized hh cyt c and cyt c″ at pH 1.9 at different phosphate concentrations, namely, 12 mM (curve a for hh cyt c and curve d for cyt c″), 1 M (curve b for hh cyt c and curve e for cyt c″), and 3 M (curve c for hh cyt c and curve f for cyt c″), as observed by circular dichroism in the far-UV region (190−240 nm, panel A), by circular dichroism in the Soret region (350−450 nm, panel B), by electronic absorption (panel C), and by resonance Raman spectroscopy (panel D). In the electronic absorption spectra the 450−700 region has been expanded 8-fold. RR experimental conditions: 406.7 nm excitation wavelength; 5 cm^{-1} resolution; 10 mW laser power at the sample. (a) 5 s/0.5 cm^{-1} collection interval; (b) 23 s/0.5 cm^{-1} collection interval; (c) 17 s/0.5 cm^{-1} collection interval; (d) 9 s/0.5 cm^{-1} collection interval; (e) 15 s/0.5 cm^{-1} collection interval; (f) 22 s/0.5 cm^{-1} collection interval. For further details, see the text.

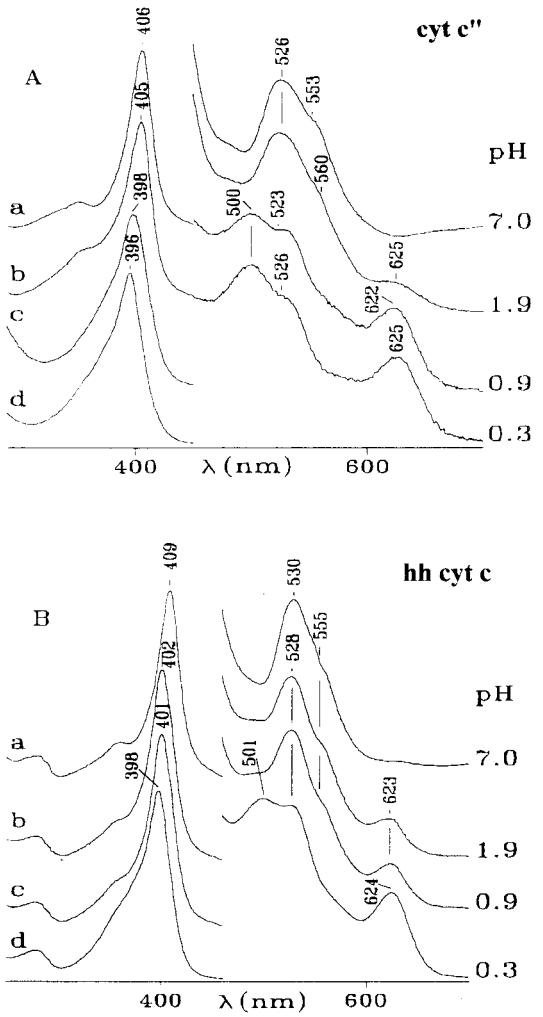

FIGURE 2: Electronic absorption spectra of oxidized cyt c″ (panel A) and of oxidized hh cyt c (panel B) at different pH values, namely, pH 7.0 (spectrum a), pH 1.9 (spectrum b), pH 0.9 (spectrum c), and pH 0.3 (spectrum d), in 3 M phosphate. The 450−700 nm region has been expanded 8-fold.

two cytochromes differ significantly. In cyt c″ a more negative ellipticity is observed at 207 nm than at 222 nm, and the opposite is observed for hh cyt c (spectra a in Figure 3A). The interpretation of this difference is not straightforward, since it might be attributed to (i) a lower percentage of α-helical structural organization in cyt c″, possibly associated with a larger flexibility of the entire molecule, and/or to (ii) a significantly different tertiary structure of the two cytochromes. In fact, in proteins with low amounts of α-helical structure, clusters of aromatic amino acids are known to affect the tertiary structure, thus influencing the far-UV CD spectrum (*15*). This might be the case for cyt c″, as the structure has not been determined yet. In the near-UV, the two proteins are distinguished mainly by the presence in hh cyt c of a double negative peak in the 280−290 nm region, which is absent in cyt c″ (spectra a in Figure 3B). Moreover, in cyt c″ a clear maximum ellipticity at 263 nm is observed, while in hh cyt c there are two positive peaks at 261 and 267 nm without a decrease of ellipticity in the 250−260 nm region, giving rise to a spectrum with an almost flat profile (spectra a in Figure 3B). Such features may also be responsible for the differences observed between the two cytochromes at pH 7.0 in the far-UV region (spectra a in

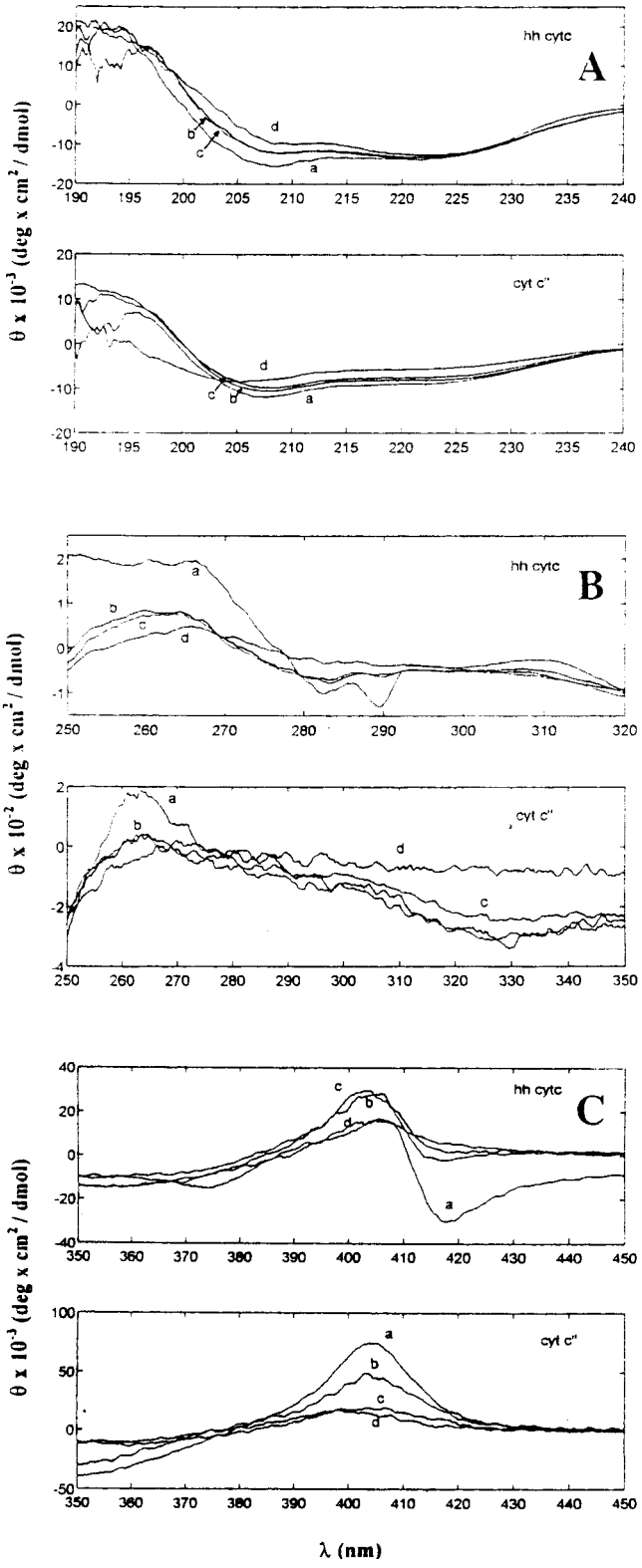

FIGURE 3: Circular dichroism spectra in 3 M phosphate of oxidized cyt c″ and hh cyt c, as indicated, in the far-UV region (190−240 nm, panel A), in the near-UV region (250−350 nm, panel B) and in the Soret region (350−450 nm, panel C). In each panel spectra are reported at pH 7.0 (spectrum a), pH 1.9 (spectrum b), pH 0.9 (spectrum c), and pH 0.3 (spectrum d). For further details, see the text.

Figure 3A), suggesting a lower α-helical content in cyt c″ associated with a more hydrophobic character of the molecule due to clusters of aromatic amino acids (*15*). In the Soret region this difference is even more drastic, being represented

by a negative ellipticity in hh cyt c at $\lambda > 410$ nm (not observed in the bis-histidyl cyt c″), which possibly reflects the presence of different residues around the heme (spectra a in Figure 3C). Furthermore, even though in both cytochromes the positive ellipticity has a maximum at around 404 nm, in hh cyt c there is also a shoulder at ≈390 nm that is not present in cyt c″.

Lowering the pH has different effects on the spectroscopic features of the CD spectra of the two cytochromes. For cyt c″, in the far-UV region a very small decrease of the negative ellipticity is observed down to pH 0.9 (spectra b and c in Figure 3A). Further lowering of pH to 0.3 brings about a blue shift of the minimum ellipticity wavelength from 207 to 203 nm (spectrum d in Figure 3A), and the spectrum, although significantly different from that of an unfolded molecule (spectrum a in Figure 1A), suggests a gross structural change of the entire molecule. Conversely, in hh cyt c lowering the pH to 0.3 induces a change in the ellipticity of the minimum dichroism at 207 nm (spectra b−d in Figure 3A), rendering the spectrum at low pH more and more similar to that of cyt c″ at neutral pH without any shift of the minimum ellipticity. Acid pH causes similar changes in the near-UV CD region of both cytochromes (Figure 3B), and at pH 0.3 the spectra appear almost flat (spectra d). In the Soret region, the negative ellipticity of hh cyt c virtually disappears at pH 1.9, while the positive ellipticity remains unchanged until pH 0.9 and decreases only upon further lowering of the pH to 0.3 (spectra b−d in Figure 3C). This is indicative of a progressive weakening of the axial heme bonds and the flattening of the heme conformation. In cyt c″ a significantly different behavior is observed. Lowering the pH induces a decrease of the ellipticity together with the appearance of a shoulder at shorter wavelengths at pH 0.9 and a blue shift of the maximum of the ellipticity to ≈395 nm at pH 0.3 (spectra b−d in Figure 3C).

To gain a better insight into the structural alterations occurring around the heme, we have recorded the RR spectra with Soret excitation under the same experimental conditions. In the high-frequency region the spectral features of the two cytochromes at pH 7.0 are very similar, indicating a predominant 6-c LS form, with a 2−4 cm^{-1} upshift of frequencies in cyt c″ (spectra a in Figure 4). It is known that for planar porphyrins an inverse correlation exists between the RR band frequencies and the metalloporphyrin core size (*16*−*18*). On the other hand, as the degree of nonplanarity of the porphyrin macrocycle increases, the size of the core decreases and the RR bands shift to lower frequencies (*19*). Therefore, an upshift of the frequencies of the 6-c LS heme of cyt c″ compared to those of hh cyt c may well be due to a partial relaxation of the heme distortion toward a more planar heme. Additional structural information on the porphyrin macrocycle may come from the low-frequency region of the RR spectra. In fact, the core size marker bands in the high-frequency RR region give information on the coordination and spin states of the heme iron. The low-frequency region can give an indication of the tertiary structure through the vibrations of the heme peripheral substituents and porphyrin out-of-plane modes. At neutral pH, hh cyt c is characterized by a very complex low-frequency region (spectra a and a′ in Figure 5), since the substituents and the out-of-plane modes become active as a consequence of a fairly distorted heme, displaying a saddle-shaped distortion. The distortion is imposed by the interactions with the surrounding protein by covalent thioether links between the β-carbon of the heme and two cysteine residues (*20*, *21*). In the cyt c″ spectrum, a large intensity decrease and frequency changes of several bands can be observed as compared to hh cyt c (spectra b and b′ in Figure 5). Similar changes were previously reported for cyt c_4 from *Pseudomonas stutzeri* (*22*), the A-state of hh cyt c (*6*), and the Met80Cys hh cyt c mutant (*23*). In particular, variation is clearly evident for the bands at 446, 567, and 730 cm^{-1} (spectra a, a′, b and b′ in Figure 5), assigned in hh cyt c to the out-of-plane modes γ_{22}, γ_{21}, and γ_5, respectively (*21*). In addition, changes are also observed for vibrations of the thioether linkage, assigned to the bands at 397 cm^{-1} [$\delta(C_\beta C_a S)$] and 692 cm^{-1} [$\nu(C-S)$] for hh cyt c. In cyt c″, this latter band becomes overlapped with the downshifted ν_7 vibration at 694 cm^{-1} (spectrum b′ in Figure 5). For the assignment of the [$\delta(C_\beta C_a S)$] vibration, two weak bands are

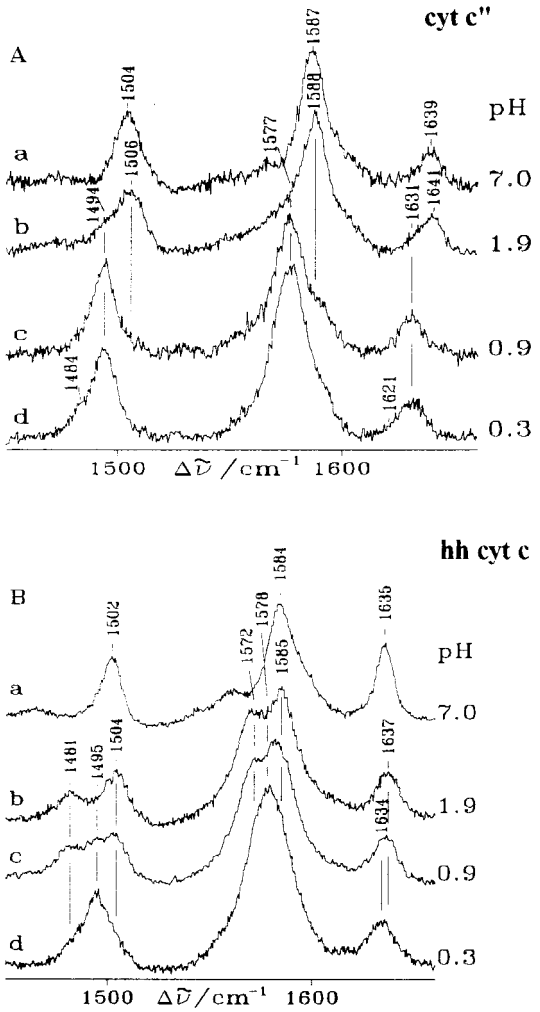

FIGURE 4: Resonance Raman spectra of oxidized cyt c″ (panel A) and hh cyt c (panel B) at different pH values, namely, pH 7.0 (spectrum a), pH 1.9 (spectrum b), pH 0.9 (spectrum c), and pH 0.3 (spectrum d) in 3 M phosphate buffer. RR experimental conditions: 406.7 nm excitation wavelength; 5 cm^{-1} resolution; 10 mW laser power at the sample (except for pH 7.0 where 20 mW laser power was used). Panel A: (a) 5 s/0.5 cm^{-1} collection interval; (b) 22 s/0.5 cm^{-1} collection interval; (c) 12 s/0.5 cm^{-1} collection interval; (d) 9 s/0.5 cm^{-1} collection interval. Panel B: (a) 6 s/0.5 cm^{-1} collection interval; (b) 17 s/0.5 cm^{-1} collection interval; (c) 27 s/0.5 cm^{-1} collection interval; (d) 7 s/0.5 cm^{-1} collection interval. For further details, see the text.

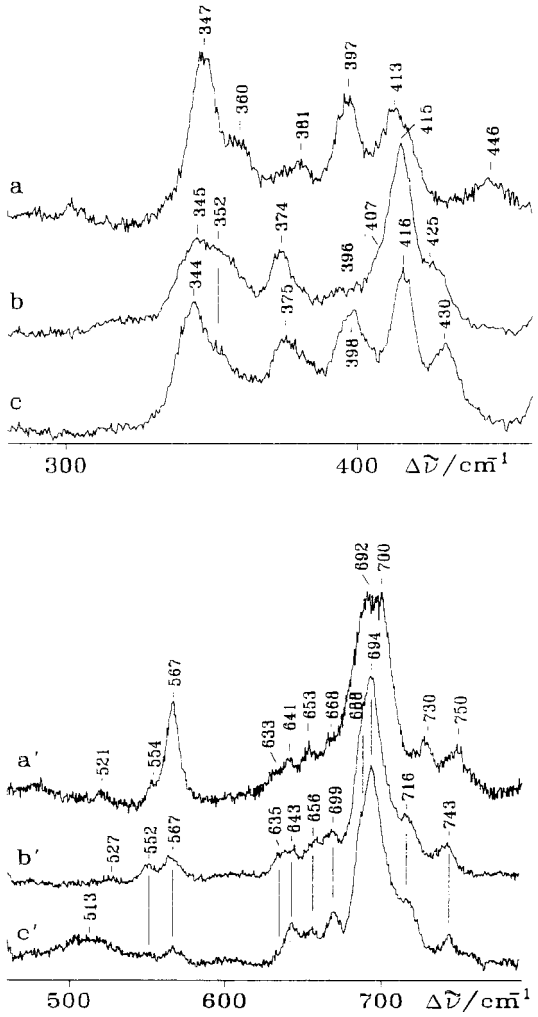

FIGURE 5: Resonance Raman spectra of oxidized hh cyt c (a, a′) at pH 7.0, cyt c″ at pH 7.0 (b, b′), and cyt c″ at pH 1.9 (c, c′) in the low-frequency region. Experimental conditions: 406.7 nm excitation wavelength; 5 cm^{-1} resolution; 15 mW (a, a′) and 12 mW (b, b′ and c, c′) laser power at the sample; (a, a′) 3 s/0.5 cm^{-1} collection interval; (b, b′) 4 s/0.5 cm^{-1} collection interval; (c, c′) 7 s/0.5 cm^{-1} collection interval.

observed in cyt c″, one at 396 cm^{-1}, which is very weak and becomes more evident with excitation at 413.1 nm (data not shown), and a shoulder at about 407 cm^{-1}. On the basis of the previous results of the imidazole complex of microperoxidase 8 (*24*), we assign the shoulder at about 407 cm^{-1} to the asymmetric stretching mode [ν_{as}(Fe−Im_2)], which is predicted to be Raman-active if the ligands are inequivalent (*25*), and the weak band at 396 cm^{-1} to the [$\delta(C_\beta C_a S)$] vibration. The latter band is, therefore, remarkably weak compared with the corresponding band observed for hh cyt c (spectra a and b in Figure 5). The existence of two inequivalent histidines bound to the heme iron in cyt c″ seems to be confirmed by previous work. They were recently identified to be His53 and His95. This latter, suggested to be the sixth ligand of cyt *c*″, is in the vicinity of a disulfide bridge, formed by Cys96 and Cys104, which represents an extra disulfide bridge extremely rare in monoheme cytochromes (*13*). Moreover, on the basis of EPR, MCD (*26*), and NMR measurements (*27, 28*), the relative orientation of the ligands was found to be nearly perpendicular, although the absolute orientation of the axial ligands cannot be well-defined in the presence of near-axial symmetry. Therefore, a different orientation of the imidazole planes of the two histidines with respect to the Fe−N pyrrole bond cannot be excluded, with one imidazole group being rotated about the normal to the heme plane to a position of low density, thus bisecting the two iron−pyrrole N bonds. This orientation of the imidazole plane will lead to a reduction in π-bonding between the Fe atom and the ligand and might be a factor contributing to the loss of one axial ligand in the ferrous form, as in the case of cyt c″ (*26*). Finally, NMR measurements showed that the two faces of the heme differ markedly with respect to water accessibility, suggesting that the proximal His (His53) resides in a rather rigid structure, practically inaccessible to water, whereas the other His (His95) is positioned in a much more open structure (*27*).

Upon lowering of the pH from 7.0 to 1.9, the 6-c LS core size marker bands in the high-frequency region are upshifted by 1−2 cm^{-1} in cyt c″ (spectrum b in Figure 4A), suggesting that at this pH the bis-histidyl coordination is still present, but the heme conformation has undergone a change involving a relaxation of the heme distortion, probably due to a weakening of the axial ligands. Moreover, a new species increases at the expense of the 6-c LS heme, which can be assigned to a 5-c HS heme, being characterized by RR frequencies at 1494 cm^{-1} (ν_3), 1577 cm^{-1} (ν_2), and 1631 cm^{-1} (ν_{10}). The 5-c HS features intensify at the expense of the 6-c LS upon further decrease of the pH to 0.9 (spectrum c in Figure 4A). At pH 0.3 (spectrum d in Figure 4A) the 6-c LS heme almost disappears and the 5-c HS heme becomes the most populated species, accompanied by a small amount of 6-c HS (characterized by ν_3 at 1484 cm^{-1} and ν_{10} at 1621 cm^{-1}). Lowering the pH from 7.0 to 1.9 also brings about changes in the low-frequency region of cyt c″ (spectra c and c′ in Figure 5). However, the intensity and frequency variations of the bands in the region between 300 and 450 cm^{-1} cannot be easily ascribed to a further decrease of the heme distortion, as suggested by the high-frequency region, since the assignment is complicated due to the overlapping contribution of 5-c HS and 6-c LS hemes. The most remarkable change observed at pH 1.9 with respect to neutral pH is the change of the relative intensity observed in the region 390−415 cm^{-1} (spectrum c in Figure 5). At pH 1.9 a strong band is observed at 398 cm^{-1} with the concomitant decrease of intensity of the band at 416 cm^{-1}. These changes might be ascribed to the downshift (and overlap with the band at 396 cm^{-1}) of the asymmetric stretching mode [ν_{as}-(Fe−Im_2)], due to the more positive charge of the His ligand. This in agreement with the fact that a more imidazolate character of the ligand in microperoxidase 8, induced by the alkaline medium, causes an upshift of this band (*24*).

In the case of hh cyt c, lowering of the pH from 7.0 to 0.3 is characterized by RR spectra that show the coexistence of three species, namely, 5- and 6-c HS and 6-c LS (Figure 4B). As found at pH 7.0, the low-spin heme is still the most abundant species at pH 1.9, but it shows RR bands upshifted by 1−2 cm^{-1} with respect to those observed at neutral pH, as previously reported (*6*). The upshift can be attributed to a relaxation of the heme distortion as in cyt c″. Identical upshifted LS bands have been recently observed in hh cyt c at neutral pH under denaturing conditions and they have been assigned to a misligated state with the native His18 and a nonnative His33 as the two axial ligands (*29*−*31*). A progressive increase of a 5-c HS heme (characterized by

bands at 1495 cm^{-1}, ν_3, and at 1578 cm^{-1}, ν_2) takes place from pH 1.9 to 0.3 at the expense of the 6-c species, present in small amounts even at the lowest pH values. The RR spectrum in the low-frequency region at pH 1.9 (data not shown) is identical to that previously reported for the unfolded protein (*31*). The tertiary structure and axial ligand interactions of the heme are relaxed and, as a consequence, the spectrum loses its complexity and the bands broaden. Since the high-frequency region shows a mixture of three species, it is difficult to analyze the low-frequency region spectrum in detail.

DISCUSSION

An overall description of the pH-linked structural transitions occurring in these two cytochromes may be attempted by exploiting the various information available from the different spectroscopic techniques.

Neutral pH. The present data show that cyt c″ at neutral pH contains a more relaxed heme in a less constrained environment, as compared to hh cyt c. We suggest that these changes result from the bis-histidine coordination and/or less steric interactions with the protein. In fact, for cyt c″, CD indicates a lower content of α-helices, possibly associated with a larger flexibility of the entire molecule, and the RR core size marker band frequencies are consistent with a partial relaxation of the heme distortion toward a more planar heme. Accordingly, the variations observed in the low RR frequency region indicate a less distorted heme in cyt c″ than hh cyt c, as a consequence of the bis-histidyl heme coordination of cyt c″ with respect to the His/Met ligands of hh cyt c. However, the absence in the CD spectrum of cyt c″ of the strong negative band at 418 nm observed for hh cyt c suggests also a reduced number of steric contacts with the protein. This band, in fact, derives from the direct interaction of the $\pi \rightarrow \pi^*$ transition of the aromatic ring of Phe82 with the $\pi \rightarrow \pi^*$ transition of the heme group (*32*). Moreover, cyt c″ shows an intensity increase and downshift of the band due to the heme propionate $\delta(C_\beta C_c C_d)$ bending modes at 374 cm^{-1}. A higher frequency of the propionyl bands is indicative of an increase in hydrogen bonding through either a strengthening of the hydrogen bond or addition of more bonds (*33, 34*). Therefore, the hydrogen-bond interactions between the propionates and the protein matrix are weaker and/or less hydrogen-bonded in cyt c″ than in hh cyt c. Unfortunately, it is not possible at this stage to draw any conclusions in this regard, since from the NMR study the two heme propionate groups appeared to have a contrasting degree of exposure to the solvent, with the heme 6-propionate being much closer to the protein surface than heme 7-propionate (*27*). It is interesting to underline that the larger flexibility and the reduced H-bond interactions displayed by cyt c″ are not contrasting with its enhanced resistance to denaturation. As a matter of fact, hyperthermophilic proteins have been shown to display a marked flexibility (*35*), contradicting the common hypothesis that rigidity of the folded state is a prerequisite for a conformational stability.

pH Effect. The pH-dependent behavior of the Fe coordination and spin state is different in the two cytochromes, as reported in Table 1. In the case of cyt c″, a direct transformation from a 6-c LS to a 5-c HS heme can be observed, while hh cyt c exhibits a 6-c HS species at intermediate pH values (pH 1.9−0.9). The presence of a 6-c HS species has also been observed previously in the A- (partially unfolded) and U-states (unfolded protein) of hh cyt c (*6, 29*) and in two mutants of hh cyt c in which Met80 has been replaced by either cysteine (*23*) or alanine (*36*). In all cases a water molecule is suggested to occupy the axial binding site of the Fe atom. Similar species have been detected by Yeh and Rousseau (*31*), who followed the kinetics of hh cyt c unfolding in guanidine hydrochloride at several pH values.

Table 1: Scheme of the Coordination−Spin-State Changes upon Lowering the pH[a]

cyt c″	pH	hh cyt c
6-c LS bis-His	7.0	6-c LS Met/His
↓		↓
5-c HS 6-c LS^{II}	1.9	6-c HS 6-c LS^{II}
↓		↓
↑5-c HS ↓6-c LS^{II}	0.9	↑5-c HS ↓6-c HS ↓6-c LS^{II}
↓		↓
↓5-c HS ↑6-c HS	0.3	↑5-c HS ↓6-c HS ↓6-c LS^{II}

[a] The most abundant species is underlined; 6-c LS^{II} corresponds to a low-spin species with less distorted heme (see text); ↑↓ The arrows indicate an increase or decrease of the species.

(A) pH 1.9. The first proton-linked transition displayed by hh cyt c seems to be complete at pH values slightly lower than 1.9. A number of observations point to a conformational change occurring at the level of the heme stereochemistry: (i) the disappearance of the negative CD maximum at 418 nm, (ii) the blue shift of the Soret band, (iii) the appearance of the CT1 band at 623 nm. Altogether, these changes can be related to the formation of both 5-c and 6-c HS species as evident from the RR spectra (see Figure 4 and Table 1). This conformational change might be associated with a partial cleavage of the Fe-Met ligand (which appears to be characterized by a $pK_a \gg 2.0$). Furthermore, the 6-c LS heme displays a 2−3 wavenumbers upshift of all the RR core size marker bands. This upshift can be attributed to a relaxation of the heme distortion. The same behavior was observed in hh cyt c at neutral pH under denaturing conditions and ascribed to a misligated state having bis-imidazolate coordination in which the axial ligands are His18, as in native hh cyt c, and His33 (*29*−*31*). The present results are in good agreement with the possibility that the 6-c LS heme present at pH 1.9 is due to a bis-histidine coordinated form where the Met ligand has been replaced by His33 (*30, 31*).

At pH 1.9 cyt c″ contains a predominant 6-c LS species, although a 5-c HS state has become visible. In this respect, it is noteworthy that the RR low-frequency region shows a downshift of the asymmetric stretching mode [$\nu_{as}(Fe-Im_2)$], which can be interpreted as due to a more positive charge of the His ligand. This suggests some modification of the heme stereochemistry and that the cleavage of the bond between the heme iron and one of the two histidyl axial residues (probably His95) has begun to occur, even if its extent is still quite limited. Some decrease in the ellipticity of the peak at 263 nm in the near-UV region and that at 406 nm in the Soret region, and the initial appearance of the electronic absorption CT1 band at 625 nm, seem to be additional structural markers for this conformational change.

(B) pH 0.9. Upon lowering the pH from 1.9 to 0.9, the 5-c HS species increases in hh cyt c at the expense of the 6-c hemes (see Table 1), and no additional variations of the structural arrangement appear to take place. This observation is confirmed by the close similarity of CD, optical absorption, and RR spectra for hh cyt c in this pH range.

Conversely, in the case of cyt c″, the pH-induced cleavage of the Fe−His95 bond (and thus the formation of a 5-c HS form) seems to be almost complete at pH 0.9. Thus, a decrease of ellipticity is induced in the Soret region of the CD spectrum with the appearance of a shoulder at shorter wavelengths. It should be noted that the decrease of ellipticity, likely related to the weakening and the cleavage of the Fe−His axial bond, is much more marked at pH 0.9 in cyt c″ than in hh cyt c. The increase in the proportion of the 5-c HS species in cyt c″ is also indicated by a blue shift of the band at 396 nm, a marked increase of the CT1 band intensity at 622 nm, and a clear downshift of the RR bands. These variations indicate that in cyt c″ the cleavage of the axial bond(s) does indeed take place at this pH. Therefore, for this Fe−His axial bond a p$K_a \cong 1.5$, and as a consequence a bond energy of $\approx$ 30 kJ/mol, is suggested. The latter value follows from the relationship of the variation of pK_a between the free and the bound histidine and the Fe−His bond energy G_{bond} (Δp$K_a \cong G_{bond}$ (in kilocalories per mole) $\times$ 0.75; see ref *37*).

(C) pH 0.3. pH 0.3 induces an additional conformational transition in hh cyt c, involving the heme axial coordination. In the Soret region, this results in a further blue shift to 398 nm of the electronic absorption band and a decrease of the positive ellipticity in the CD spectrum. This latter is indicative of a progressive weakening of the axial heme bonds and the flattening of the heme conformation. Therefore, a major tertiary structural change appears to have occurred, which probably also gives rise to the spectroscopic changes of the CD spectra in the far- and near-UV region. This conformational transition concerns a large fraction of the molecules, and an analysis of the RR spectra indicates that it leads to mainly 5-c HS species with minor fractions of both 6-c species. The spectroscopic changes may reflect the cleavage of the misligated Fe−His33 bond, which appears to display a p$K_a \cong 1.0$.

In the case of cyt c″, at pH 0.3, the blue shift of the maximum ellipticity to $\approx$395 nm and the changes in the far- and in the near-UV regions indicate that at pH < 1.0 a new stereochemical arrangement of the heme surroundings occurs, which is never observed in the case of hh cyt c. At this very low pH becomes evident a new species that, on the basis of the RR, electronic absorption, and CD spectra, can be assigned to a 6-c HS heme. It is probable that this form results from the cleavage of the second axial bond between the heme iron and the N_ϵ of the imidazole of His53, with the consequent coordination of a H_2O molecule, leading to a bis-aquo species. However, this event might be the consequence of a major conformational change of the whole protein, as suggested by the drastic spectral transitions occurring in the far- and near-UV CD spectra. This being the case, it is noted that the Fe−His53 proximal bond in oxidized cyt c″ has a p$K_a \leq 1.0$, thus somewhat lower than that displayed by the Fe−His95 bond, corresponding to a higher bond energy by $\approx$10 kJ/mol. Further, this behavior appears to be compatible with the possibility of a concerted cleavage of the two axial bonds. This is suggested by the cooperative variation of the reduction rates for cyt c″ over the pH range between 1 and 2 (*14*), such that the rupture of the Fe−His95 bond facilitates the subsequent weakening (and cleavage) of the Fe−His53 bond.

In conclusion, the pH-dependent evolution of the structural changes in the two cytochromes appears to derive from two factors. The first factor is their different structural organization. In hh cyt c the more compact heme surroundings with respect to cyt c″ should prevent the immediate formation of a 5-c HS at pH 1.9. However, a different polarity of the distal cavity between the two cytochromes cannot be ruled out, since the coordination of a water molecule to the heme iron depends also on the stabilization of the ligand by polar residues. The second factor is the axial ligands, as has been reported previously (*8*). In particular, the variation of the energy of the axial bonds, which is related to the nature of the heme ligands, may be responsible for the appearance of different 6-c and 5-c forms, which is accompanied by structural changes at the level of the protein moiety. Thus, the different bond energy of the Fe−Met80 and the Fe−His33 bonds could be responsible for the appearance of a misligated state in hh cyt c at low pH. On the other hand, in cyt c″ communication between the two His ligands through the Fe atom may be possible, which brings about the formation of an unstable 5-c heme. This subsequently evolves toward a bis-aquo form in which also the second axial bond is broken in a concerted fashion.

REFERENCES

1. Goto, Y., Takahashi, N., and Fink, A. L. (1990) *Biochemistry 29*, 3480−3488.
2. Jeng, M.-F., Englander, S. W., Elove, G. A., Wand, A. J., and Roder, H. (1990) *Biochemistry 29*, 10433−10437.
3. Jeng, M.-F., and Englander, S. W. (1991) *J. Mol. Biol. 221*, 1045−1061.
4. Kuroda, Y., Kidokoro, S., and Wada, A. (1992) *J. Mol. Biol. 223*, 1139−1153.
5. Goto, Y., Hagihara, Y., Hamada, D., Hoshino, M., and Nishii, I. (1993) *Biochemistry 32*, 11878−11885.
6. Jordan, T., Eads, J. C., and Spiro, T. G. (1995) *Protein Sci. 4*, 716−728.
7. Marmorino, J. L., and Pielak, G. J. (1995) *Biochemistry 34*, 3140−3143.
8. Hamada, D., Kuroda, Y., Kataoka, M., Aimoto, S., Yoshimura, T., and Goto, Y. (1996) *J. Mol. Biol. 256*, 172−186.
9. Marmorino, J. L., Lehti, M., and Pielak, G. J. (1998) *J. Mol. Biol. 275*, 379−388.
10. Goto, Y., Calciano, L. J., and Fink, A. L. (1990) *Proc. Natl. Acad. Sci. U.S.A. 87*, 573−577.
11. Hagihara, Y., Tan, Y., and Goto, Y. (1994) *J. Mol. Biol. 237*, 336−348.
12. Costa, H. S., Santos, H., Turner, D. L., and Xavier, A. V. (1992) *Eur. J. Biochem. 208*, 427−433.
13. Klarskov, K., Leys, D., Backers, K., Costa, H. S., Santos, H., Guisez, Y., and Van Beeuman, J. J. (1999) *Biochim. Biophys. Acta 1412*, 47−55.
14. Coletta, M., Costa, H., De Sanctis, G., Neri, F., Smulevich, G., Turner, D. L., and Santos, H. (1997) *J. Biol. Chem. 272*, 24800−24804.
15. Manning, M. C., and Woody, R. W. (1989) *Biochemistry 28*, 8609−8613.
16. Hoard, J. (1973) *Ann. N.Y. Acad. Sci. 206*, 18−31.
17. Spaulding L. D., Chang C. C., Yu, N.-T., and Felton, R. H. (1975) *J. Am. Chem. Soc. 97*, 2517−2525.

18. Choi, S., Spiro, T. G., Langry, K. C., Smith, K. M., Budd, D. L., and La Mar, G. N. (1982) *J. Am. Chem. Soc. 104*, 4345−4351.
19. Sparks, L. D., Anderson, K. K., Medforth, C. J., Smith, K. M., and Shelnutt, J. A. (1994) *Inorg. Chem. 33*, 2297−2302.
20. Bushnell, G. W., Louie, G. V., and Brayer, G. D. (1990) *J. Mol. Biol. 214*, 585−595.
21. Hu, S., Morris, I. K., Singh, J. P., Smith, K. M., and Spiro, T. G. (1993) *J. Am. Chem. Soc. 115*, 12446−12458.
22. Nissum, M., Karlsson, J.-J., Ulstrup, J., Jensen, P. W., and Smulevich, G. (1997) *J. Biol. Inorg. Chem. 2*, 302−307.
23. Smulevich G., Bjerrum, M. J., Gray, H. B., and Spiro, T. G. (1994) *Inorg. Chem. 33*, 4629−4634.
24. Othman, S., Le Lirzin, A., and Desbois, A. (1994) *Biochemistry 33*, 15437−15448.
25. Spiro, T. G., and Li, X. Y. (1988) in *Biological Applications of Raman spectroscopy* (Spiro, T. G., Ed.) pp 1−37, Wiley, New York.
26. Berry, M. J., George, S. J., Thomson, A. J., Santos, H., and Turner, D. L. (1990) *Biochem. J. 270*, 413−417.
27. Costa, H. S., Santos, H., and Turner, D. L. (1993) *Eur. J. Biochem. 215*, 817−824.
28. Costa, H. S., Santos, H., and Turner, D. L. (1996) *Eur. Biophys. J. 25*, 19−24.
29. Takahashi, S., Yeh, S.-R., Das, T. K., Chan, C.-K., Gottfried, D. S., and Rousseau, D. L. (1997) *Nat. Struct. Biol. 4*, 44−50.
30. Colon, W., Wakem, L. P., Sherman, F., and Roder, H. (1997) *Biochemistry 36*, 12535−12541.
31. Yeh, S.-R., and Rousseau, D. L. (1999) *J. Biol. Chem. 274*, 17853−17859.
32. Pielak, G. J., Oikawa, K., Mauk, A. G., Smith, M., and Kay, C. M. (1986) *J. Am. Chem. Soc. 108*, 2724−2727.
33. Gottfried, D. S., Peterson, E. S., Sheikh, A. G., Wang, J., and Friedman, J. M. (1996) *J. Phys. Chem. 100*, 12034−12042.
34. Cerda-Colon, J. F., Silfa, E., and Lopez-Garriga, J. (1998) *J. Am. Chem. Soc. 120*, 9312−9317.
35. Jaenicke, R. (2000) *Proc. Natl. Acad. Sci. U.S.A. 97*, 2962−2964.
36. Bren, K. L., and Gray, H. B. (1993) *J. Am. Chem. Soc. 115*, 10382−10383.
37. Traylor, T. G., Deardurff, L. A., Coletta, M., Ascenzi, P., Antonini, E., and Brunori, M. (1983) *J. Biol. Chem. 258*, 12147−12148.

BI000266I